New Horizons in Earth Reinforcement – Otani, Miyata & Mukunoki (eds)

Geosynthetic encased stone columns in soft clay

S.R. Lo
University of New South Wales, ADFA Campus, Canberra Australia

J. Mak
Roads and Traffic Authority, New South Wales, Sydney, Australia

R. Zhang
University of New South Wales, ADFA Campus, Canberra Australia

ABSTRACT: A preliminary numerical study on the reinforcing effects of stone columns in a very soft clay deposit was undertaken. The reinforcing effect of stone columns is dependent on the mobilization of confining stress by the surrounding soil. For very soft or weak soil, this confining stress may be augmented by the use of geosynthetic encasement. This hypothesis was examined by a preliminary numerical study. The findings of this preliminary study highlighted the potential benefit of reinforcing the stone columns by geosynthetic encasement.

1 INTRODUCTION

Stone columns have been used extensively to improve the bearing capacity of weak soils. They can be used in a small cluster as vertical load bearing members similar to piles. Alternatively, a large number of stone columns can be used to strengthen a weak soil stratum for supporting a fill structure such as a road embankment. This paper is for the latter application. The bearing capacity of a stone column can be assessed based on design guidelines such as FHWA (1983). Stone columns can also be used to reduce settlement. Such an application is useful for supporting a road embankment section that leads to a piled abutment. Oh et al (2007) reported the settlement performance of a 4 m high trial embankment constructed on soft estuarine clay improved by stone columns. The observed settlement at natural ground level (over a period of 457 days) of the stone columns treated section was only slightly less than that of the untreated section. The clay of this site, which is located in south-east Queensland, Australia, is very compressible, with a compressibility Index, C_C, exceeding 1.5. It is noted that there is no stiff crust overlying the soft clay layer, and water table is at a depth of 0.5 m. It was hypothesized that the stone columns bulged and compressed excessively because of lack of confinement. It is pertinent to note that such ground condition is not uncommon for estuarine deposits along the coast between northern New South Wales to south-east Queensland.

The observed settlement performance of the above trial embankment sections founded on a very soft clay strengthen with stone columns raises the question about the effectiveness of stone columns in reducing settlement of very weak deposits. The paper presents a preliminary numerical study on the performance of stone columns in very soft soil. The potential benefits of reinforcing stone column with a geosynthetic encasement are highlighted by this preliminary study.

2 THEORETICAL CONSIDERATIONS

2.1 *Stone columns as reinforcing elements*

Stone columns can be viewed as compressive reinforcements in a matrix of weak soils. They are constructed from stones which behave like a granular geo-material. Therefore, the strength and stiffness of a stone column is dependent on effective confining stress provided by the surrounding soil. A high effective confining stress can normally be induced by the installation process, with the stones being expanded against the surrounding soil. For very soil clay, and maybe stone columns installed at wider spacing, this may not be achieved effectively. The mobilization of additional confining stress on the stones, and thus the generation of higher bearing capacity, can still be realized during or after placement of fill as axial straining of the stones is always accompanied by lateral expansion against the surrounding clay. However, the stone columns may not be adequately effective in reducing settlement of the fill structure.

As one of the key issues is the generation of adequate confining stress to the stones prior to or

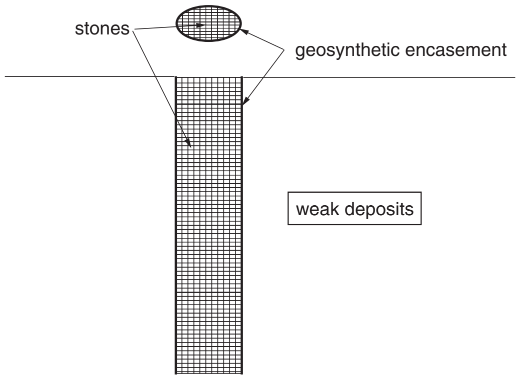

Figure 1. Geosynthetic encased stone column.

during imposition of axial loading from the fill, it was decided to examine the option of encasing/wrapping the stone with geosynthetic reinforcement as illustrated in Figure 1. This geosynthetic encasement can be provided by a geogrid-geotextile composite. The geogrid functions as the reinforcement whereas the geotextile prevents loss of stones into the surrounding soft clay.

2.2 *Contribution of geosynthetic encasement*

Unless stated to the contrary, all stresses on geomaterials are effective stress. The radial stress in acting on the stone column, σ_{rs}, can be expressed in terms of the radial stress of the surrounding clay, σ_r, and the hoop tension, T, in the geogrid encasement as illustrated Figure 2.

$$\sigma_{rs} = \sigma_r + T/R \quad (1)$$

where R is the radius of the stone column. The second term can be view as the additional effective radial stress due to the geogrid encasement. Both T and σ_r can be decomposed into two parts, the initial value (ie after stone column installation) and the increase due to placement of fill and time dependent deformation. Therefore, Eqn (1) can be re-written as

$$\sigma_{rs} = \sigma_r(i) + T(i)/R + \Delta\sigma_r + \Delta T/R \quad (2)$$

where (i) denotes the initial (as-installed) state, and "Δ" denotes increase due to loading.

To enable the stones to develop adequate strength and stiffness, σ_{rs} has to be of adequate magnitude. If an adequately high $\sigma_r(i)$ can be generated, then both T(i) and ΔT are not needed. Indeed the value of $\Delta\sigma_r$ will also be low as the axial strain, and thus the radial expansion, of the stone column is small. However, one

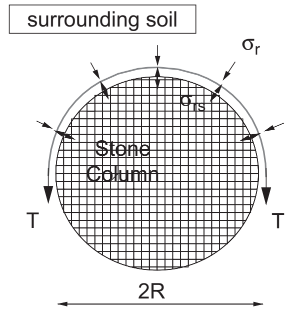

Figure 2. Hoop tension and radial stress in stone column.

can compensate for a low $\sigma_r(i)$ value, say due to the surrounding clay being very soft, by the introduction of a significant T(i) value. The presence of a significant T(i) value automatically implies additional contribution to effective radial stress by the ΔT term. An initial tension in the geogrid encasement, T(i), can be induced by installing a stone column using the casing method, plus slightly "undersizing" the prefabricated geogrid encasement and controlling the compaction of the stone. This is more an in-principle statement on the possibility of installing a geogrid-encased stone column. The aim of this paper is to explore the potential beneficial effect of geogrid encasement.

Immediately after the imposition of fill loading imposed, the stone columns perform only a small reinforcing role as most of the total stress is taken by pore water pressure in the clay. It is only with dissipation of pore water pressure with time that the clay will settle and the weight of the fill will "arch over" to the stone column. During this process, the stone column will strain both axially and radially, the latter leading to both ΔT and $\Delta\sigma_r$. Some of the fill loading will still be transferred to the clay as effective stress and this also leads to $\Delta\sigma_r$. Therefore, the mechanism involves the interaction of the stone columns and dissipation of pore water pressure of the surrounding clay. The latter is a coupled process between mechanical behaviour (as governed by effective stress principle) and flow of pore water (as governed by Darcy law). In order to take into account all these complicated interaction, a fully coupled finite element analysis of a unit cell using elasto-plastic soil models will be conducted as explained in a subsequent section.

3 UNIT CELL ANALYSIS

We examined the condition where the fill area was large relative to the thickness of the soft clay and that a large number of stone columns were installed. With the exception of the stone columns near the edges, we can idealise the problem by a unit cell as illustrated in

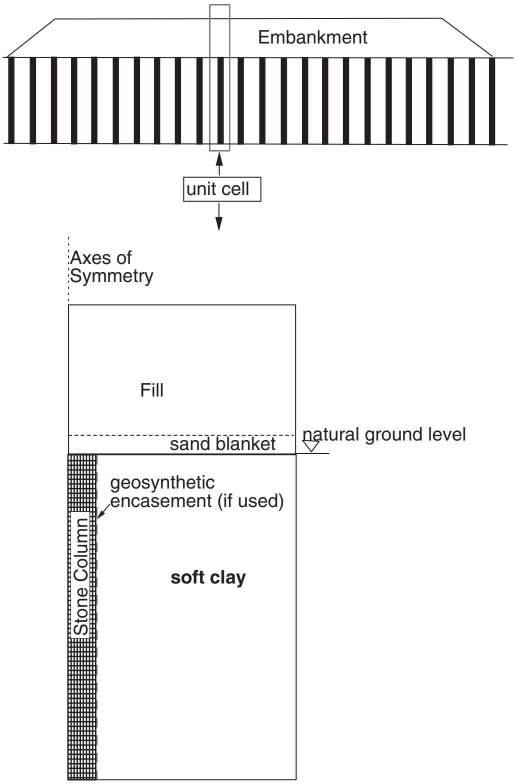

Figure 3. Unit cell.

Table 1. Parameters for unit cell analysis.

Item	Dimension
Embankment elevation	4.0 m
Sand blanket thickness	1.0 m
Diameter of stone column	0.6 m
Unit cell radius	2.0 m
Depth of ground water table	0.0 m
Thickness of soft clay	10.0 m

Figure 3. The top of the clay layer was modelled as a free draining boundary, whereas the edge of the unit cell was modeled as impermeable.

Placement of the embankment fill in layers was simulated in the analysis. Stone column construction commenced after the construction of a sand blanket. This was modeled by activating the hoop tension of the geogrid after placement of the sand blanket.

The assumed dimensions for the analysis were listed in Table 1. It was recognized that this was a rather extreme condition, but it served to highlight the beneficial effect, if any, of geogrid encasement.

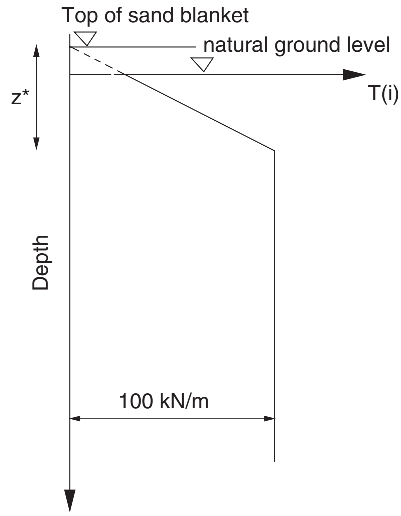

Figure 4. Initial hoop tension.

Two stone column configurations were analysed, one without geogrid and the other with geogrid encasement. For both configurations, the dissipation of pore water pressure and thus development of settlement after the completion of embankment was tracked numerically for 10 years.

3.1 *Modelling of geogrid encasement*

The geogrid, if used, was modeled as an anisotropic elastic material with a hoop stiffness of 2000 kN/m. The stiffness in the vertical direction was assigned a low value so that it will not provide any significant vertical support to the fill loading. The initial hoop tension, T(i), was also assigned a value of 100 kN/m except with the top zone where the value of T(i) was limited by triaxial extension failure of the stones.

From Eqn (2), the initial radial stress acting in the stone, $\sigma_{rs}(i)$, is given by:

$$\sigma_{rs}(i) = \sigma_r(i) + 3.33T(i) \tag{3}$$

The condition of failure in triaxial extension means $\sigma_{rs}(i)$ is given by the following equation:

$$\sigma_{rs}(i) = K_p \sigma_{zs}(i) \tag{4}$$

where $\sigma_{zs}(i)$ is the in-situ vertical stress (due to self weight of stones), $K_p = (1 + \sin\phi)/(1 - \sin\phi)$, and ϕ is the friction angle of the stones. Therefore, the distribution of T(i) is given in Figure 4, where T(i) attained the allowable value of 100 kN/m at a depth z* measured from top of sand blanket.

Assuming water table is at natural ground level, z* given by:

$$z^* = \frac{333/K_p - \gamma t_s}{\gamma'\left(1 - \rho K_0/K_p\right)} + t_s \quad (5)$$

where γ' = effective unit weight of stones, γ = bulk unit weight of stones, ρ = ratio of effective unit weight of clay to that of stones = 0.65, t_s = thickness of sand blanket = 1 m, K_o = at-rest earth pressure coefficient of the soft clay = 0.535.

3.2 *Modelling of soft clay*

The soft clay was modeled by the modified Cam-Clay model. The relevant Cam-Clay soil parameters are: $\lambda = 0.65$, $\kappa/\lambda = 0.1$, M = 1.1, $e_{cs} = 4.0$.

In-situ stress was assigned based on an effective unit weight of 6 kN/m^3 and K_o = 0.535. As the analysis modeled the coupled process of time dependent dissipation of pore water pressure, permeability parameters were also needed. The horizontal permeability of the soft clay was 2.3×10^{-10}m/s, and with a horizontal to vertical permeability ratio of two. The above parameters were typical of very soft estuarine clay deposits of a road construction site along the coast of northern New South Wales, Australia. A typical undrained shear strength profile was also assumed. From this undrained strength profile, it was inferred, following Potts and Ganendra (1991), that the top 3 m was overconsolidated ever though the soil was soft. For this top 3 m, the inferred value of p'_c, the stress at the apex of the Cam-Clay ellipse, was 69 kPa at natural ground level reducing to 40 kPa at 3 m depth.

3.3 *Modelling of fill*

The fill was modeled as a Mohr Coulomb elastic-plastic material. The parameters adopted for the analysis were: unit weight = 20 kN/m^3, $\phi = 30°$, c = 20 kPa, E = 30 MPa and $\psi = 5°$, where E = Young's modulus and ψ = dilatancy angle.

3.4 *Modelling of stone columns*

The stones column was modeled as a free draining material with $\phi = 45°$, c = 5 kPa. A small cohesion of 5 kPa is used to suppress potential numerical problems and to take into account, approximately, that the failure surface of stones is curved.

Two different approaches, depending on whether geogrid encasement was used or not, were needed to complete the modeling of the mechanical behaviour of a stone column. For both approaches, the influence of confining stress on stiffness needs to be captured.

3.4.1 *The case of no-geogrid encasement*

It was assumed that high effective radial stress would not be generated and thus σ_{rs}(i) is less than σ_{zs}(i), the in-situ vertical stress (due to self weight of stones). Therefore, the major principal stress is initially vertical and will remain closer to vertical during and after placement of fill. The stones were modeled by the Duncan-Chang non-linear elastic equation for tangential Young's modulus, E.

$$E = K\left(\frac{\sigma_3}{p_a}\right)^n p_a\left(1 - r_f S\right)^2 \quad (6)$$

Where K, n, and r_f are non-dimensional parameters for the Duncan-Chang model, σ_3 is the minor principal stress, p_a is the standard atmospheric pressure in consistent unit, and S is a function of the stress state, ϕ and c. S reflects the mobilization of the shear strength of soil and takes a value in the range of 0 to 1. The parameters for the stones were conservatively taken as: K = 1000, n = 0.6, r_f = 0.7.

3.4.2 *For the case with geogrid encasement*

The initial hoop tension, T(i) is related to an initial radial stress stones, σ_{rs}(i) by Eqn (3). Therefore, together with the distribution of T(i) shown in Figure 4 (as established from earlier Section 3.2) and still using $\phi = 45°$ for the stones, the distribution of initial radial stress in the stones, σ_{rs}(i), is given in Figure 5.

It is evident that $\sigma_{rs}(i) > \sigma_{zs}(i)$. Thus the major principal stress is initially horizontal. The imposition of loading on the stone column leads to an increase in σ_{zs}. During the early phase of loading, the stress states in the stones still satisfied the condition of $\sigma_{rs} > \sigma_{zs}$. Thus the stress ratio decreased with imposition of column load and the behaviour of the stones corresponded to that of "unloading"., and could be approximated by the initial Young's modulus, E_o given by:

$$E_0 = K\left(\frac{\sigma_{rs}}{p_a}\right)^n p_a \quad (7)$$

During the later phase of loading when $\sigma_{zs} > \sigma_{rs}$, imposition of additional load on the stone column led to an increase in stress ratio. Furthermore, the major principal stress direction was closer to vertical. The Duncan-Chang equation (Eqn (6)) may apply. The tangential Young's modulus will be less than E_o, and is a function of the stress state of the stones. It has a minimum value of $E_0{*}(1 - r_f)^2$. As a first approximation, we use an "average" Young's modulus taken as 50% of E_o. Therefore:

$$\bar{E} = 0.5K\left(\frac{\sigma_{rs}}{p_a}\right)^n p_a \quad (8)$$

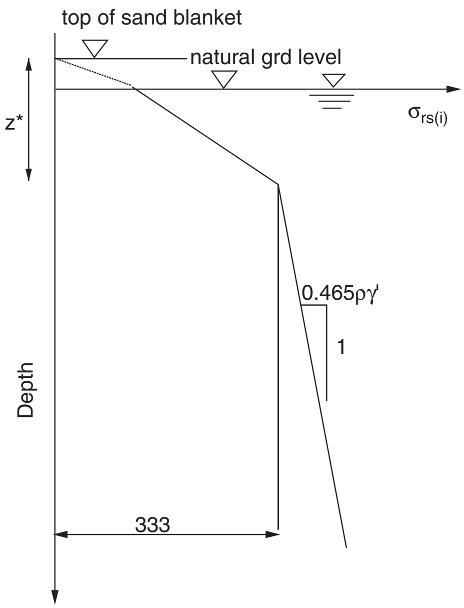

Figure 5. Initial radial stress in stone column.

Noting that $\sigma_{rs} > \sigma_{rs}(i)$, an additional conservative simplification was made by replacing σ_{rs} with $\sigma_{rs}(i)$. The average Young's modulus is given by:

$$\bar{E} = 0.5K\left(\frac{\sigma_{rs}(i)}{p_a}\right)^n p_a \tag{8a}$$

Note that $\bar{E}$ is a function of depth and initial hoop tension in the geogrid. It was used in conjunction with the Mohr Coulomb elastic-plastic model with an non-associative flow rule. The dilatancy angle, ψ, is taken as 0.33ϕ.

4 RESULTS OF FINITE ELEMENT ANALYSIS

4.1 *Settlement*

The developments of settlements with time for the two configurations are compared in Fig. 6 at top of stone column. It is evident that the settlement increases with time because the arching-over of the imposed load to the stone column is related to the settlement of the soft clay.

For the condition of nil strengthening by stone columns, the final settlement calculated based on conventional 1D consolidation was 1.55 m. Therefore, both stone column configurations reduced settlement by a significant amount. The without-geogrid stone

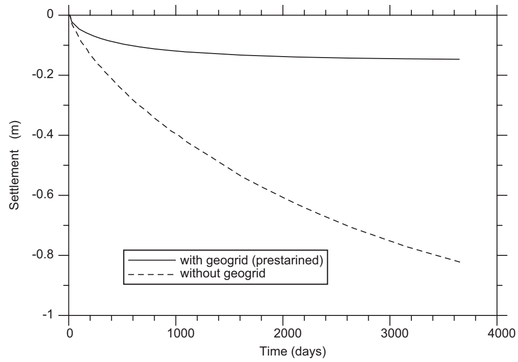

Figure 6. Development of settlement with time.

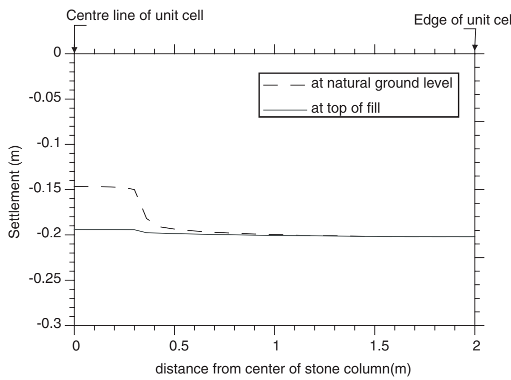

Figure 7. Settlement profile.

column configuration had a computed settlement in excess of 800 mm in 10 years. The stone column with geogrid encasement had a considerably lower settlement, just slightly in excess of 150 mm in 10 years. For the configuration without geogrid, settlement is still increasing at a considerable rate after 10 yr. However, for the with-geogrid configuration, the 10-yr settlement of approaches closely to an asymptotic value. This aspect will be examined at a later sub-section with reference axial force in the stone column.

The settlement profiles at natural ground level and at top of fill are compared in Fig. 7. It was recognised that the natural ground surface already settled by a small amount at completion of fill placement, ie when settlement of top of fill just commenced. Therefore, the settlement profile at top of fill presented in Fig. 7 was shifted so that can be compared to that at natural ground level. The profile at natural ground level manifested a bump of 50mm over a distance of 0.2 m. This is believed to be due to the stiffening effect of the geogrid encased stone column. However, at top of fill, the settlement profile was smooth.

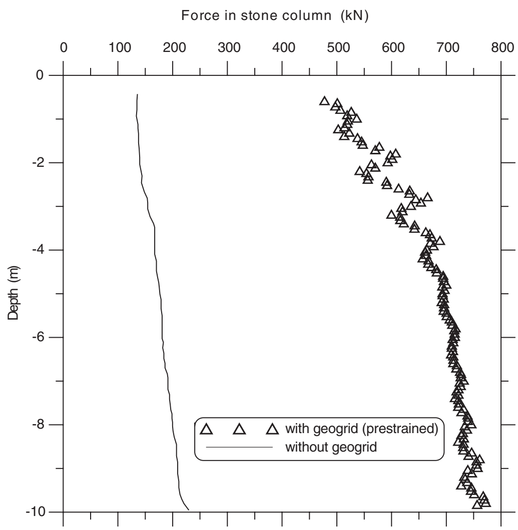

Figure 8. Force in stone column.

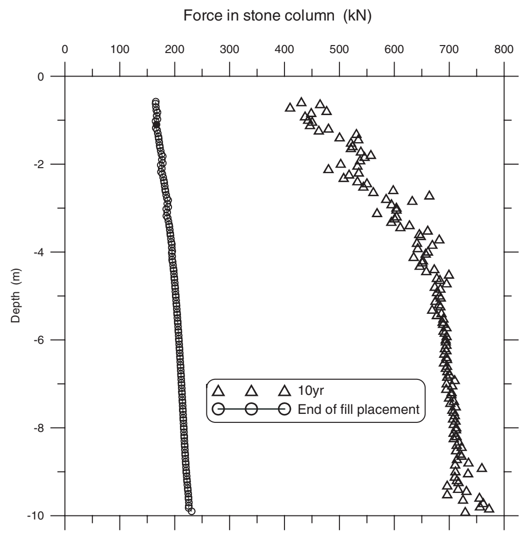

Figure 9. Development of column force with time (with geogrid encasement).

4.2 *Axial force in stone column*

The load transfer to the stone column was illustrated in Fig. 8 which showed the variation of axial load on stone column with depth. The stone column with geogrid encasement had a significantly higher load compared to that of without-geogrid configuration. For both configurations, the axial force in the stone column increased with depth. This was due to the drag-down force induced by the settlement of the surrounding clay relative to the stone column. The stiffer geogrid encased stone column attracted higher drag-down force and thus manifested a greater increase of axial force with depth, as evident from Figure 8.

The distribution of column load, for the geogrid encased configuration, at 10 year is compared to that at end of fill placement in Fig. 9. The stone column attracted an increasing amount of load with time. This means that the effective stress in the soft clay will attain an asymptotic value via two mechanism, dissipation of pore water pressure and increase in transfer of load to the stone column. The latter mechanisms will lead to the settlement reaching an asymptotic value faster for the geogrid encased configuration as illustrated in Fig. 6.

5 CONCLUSION

A preliminary numerical study was undertaken to examine the reinforcing role of stone columns in soft clay. For very soft clay, the results of the analysis indicated that the surrounding clay may not provide adequate confining stress to the stone columns. Thus the stone columns may not be effective in reducing settlement. This simplified numerical analysis suggested that if the hoop tension in the geosynthetic encasement can be mobilized upon stone column installation, then it will induced significant confining stress onto the stones despite the surrounding soil being very soft, which in turn enhance the reinforcing role of the stone columns.

ACKNOWLEDGEMENT

The last author acknowledged the financial supported provided by the the Cheung Kong Endeavour Award and the University College Postgraduate Research Award Scholarship, The University of New South Wales. The opinions expressed in this paper are solely those of the authors.

REFERENCES

FHWA (1983) Design and construction of stone columns. FHWA Report No. RD-83/026, 194p.

Oh E.Y.N., Balasubramaniam A.S., Bolton M., Chai G.W.K., and Huang M. (2007) Behaviour of a highway embankement on stone columns improved estuarine clay. 567–572.

Potts D.M. and Ganendra D. 1991. Discussion on “Finite element analysis of the collapse of reinforced embankment on soft ground by Hird C.C., Pyrah I.C., Russel D.”. *Geotechnique*, **41[4]:**627–630.